frontiers in Materials

ORIGINAL RESEARCH
published: 22 August 2019
doi: 10.3389/fmats.2019.00205

Nanoindentation Characterization on Microhardness of Micron-Level TiC and TiB Reinforcements in *in-situ* Synthesized (TiC+TiB)/Ti-6Al-4V Composite

Yan Wen[1,2*†], *Tingting Guo*[3*†], *Yuangui Zhou*[4], *Huiping Bai*[4] *and Zhou Wang*[1,2]

[1] *Hubei Key Laboratory of Advanced Technology for Automotive Components, School of Automotive Engineering, Wuhan University of Technology, Wuhan, China,* [2] *Hubei Collaborative Innovation Center for Automotive Components Technology, Wuhan, China,* [3] *Institute for Frontier Materials, Deakin University, Geelong, VIC, Australia,* [4] *Wuhan Branch of Baosteel Central Research Institute, Wuhan, China*

OPEN ACCESS

Edited by:
Lechun Xie,
Wuhan University of Technology, China

Reviewed by:
Ke Zhan,
University of Shanghai for Science and Technology, China
Jian Wang,
Xihua University, China

***Correspondence:**
Yan Wen
gubi2008@whut.edu.cn
Tingting Guo
tingting.guo@research.deakin.edu.au

[†] *These authors have contributed equally to this work*

Specialty section:
This article was submitted to Structural Materials, a section of the journal Frontiers in Materials

Received: *06 July 2019*
Accepted: *08 August 2019*
Published: *22 August 2019*

Citation:
Wen Y, Guo T, Zhou Y, Bai H and Wang Z (2019) Nanoindentation Characterization on Microhardness of Micron-Level TiC and TiB Reinforcements in in-situ Synthesized (TiC+TiB)/Ti-6Al-4V Composite. Front. Mater. 6:205. doi: 10.3389/fmats.2019.00205

The microhardness of micro-level TiC and TiB reinforcements in *in-situ* synthesized (TiC+TiB)/Ti-6Al-4V composite were investigated independently by spherical nanoindentation. The morphology of indentation on the matrix, reinforcements and the reinforcement/matrix interfaces were characterized by scanning electron microscope (SEM). The influence of cracks on the load-displacement curves and microhardness were analyzed and discussed. The microhardness of TiC and TiB were calculated from the load-displacement curves on reinforcements without cracks. The average microhardness of TiC and TiB in this composite were 24.1 and 19.6 GPa, respectively, which agreed with the values in other composites and coatings. These results verified that the nanoindentation method was a very useful method to characterize the microhardness of micron-level reinforcements in discontinuous metal matrix composite.

Keywords: microhardness, nanoindentation, reinforcements, load-displacement curves, TiC, TiB

INTRODUCTION

Due to the high specific strength, good specific modulus, and high strength at elevated temperature, titanium matrix composites (TMCs) have wide application prospects in the fields of aerospace, automobile and other industries (Tjong and Ma, 2000; Zhang et al., 2006, 2018; Huang et al., 2015; Zhang and Attar, 2016; Huang and Geng, 2017; Xie et al., 2018a; Wang et al., 2019; Zhang and Chen, 2019). Nowadays, the popular method of manufacturing TMCs is the *in-situ* technology, which is simple, useful and overcomes the shortcoming of traditional manufacture techniques (Lu et al., 2001b; Zhang and Attar, 2016; Huang and Geng, 2017; Wang et al., 2017). Regarding the shapes of reinforcements, they include the continuous fibers, whiskers and particles, and the composite reinforced with whiskers or particles possess the isotropic behaviors, ease of fabrication and low cost comparing with the continuous fibers (Saito et al., 1995; Tjong et al., 1999; Tu et al., 2002; Feng et al., 2015). As representative reinforcements, TiC particles and TiB whiskers draw much attention because of their good properties such as high modulus, high chemical and thermal stability, clean interface without any unfavorable reaction with matrix, and the similar density and thermal expansion coefficient to matrix

(Schuh and Dunand, 2001; Wagoner Johnson et al., 2003; Wei et al., 2011; Koo et al., 2012; Rastegari and Abbasi, 2013). The TiC and TiB co-reinforced TMC of (TiB+TiC)/Ti-6Al-4V has been fabricated and investigated, and some valuable results have been obtained (Lu et al., 2001c; Geng et al., 2003; Wang et al., 2005; Sun et al., 2012; Xie et al., 2012, 2018b). However, most research focused on the macroscopical mechanical properties of this composite, few work about the micromechanical properties of micro-level TiC and TiB reinforcements can be excavated because of the small sizes and diversified shapes. Thus, the aim of this work is to explore the microhardness of micro-level TiC and TiB reinforcements.

Nanoindentation method is effective to characterize the microhardness on thin films and coatings (Oliver and Pharr, 1992, 2004; Donohue et al., 2012; Xie et al., 2014). Regarding the mechanical properties of TiC and TiB investigated by nanoindentation, the single reinforcement of TiC or TiB has been investigated. In terms of TiC, the hardness of TiC single crystal was measured with the values between 20 and 32 GPa, and the indentation critical stress intensity factors were in the range of 1.5–3.6 MPa $m^{1/2}$ (Maerky et al., 1996). The nanomechanical properties of TiC thin films deposited on silicon (100) substrates were investigated, and the hardness and Young's modulus ranged from 20.56 to 23.64 GPa, and from 264.81 to 272.06 GPa (Fang et al., 2004). The hardness and Young's modulus were 4.19 and 234 GPa respectively for CoCrCuFeNi(Ti, $B_4C)_{0.1}$, and the values only revealed the average hardness of (Ti, $B_4C)_x$ coating, not the values of single TiC or TiB_2 (Cheng et al., 2015). A nanoindentation simulation was conducted to evaluate the hardness of TiC using the embedded atom method, and the hardness of TiC was 15.88 GPa in the fundamental conditions of temperature and pressure (Sekkal et al., 2005). In terms of TiB, the local modulus and hardness of TiB phase were measured using nanoindentation, and the average values were 450 and 30 GPa, respectively (Banerjee et al., 2004). A massive array indentation approach was proposed to investigate the *in-situ* elastic properties of individual phases within a multiphase microstructure (Constantinides et al., 2006). The Ti/TiB composite with 95% volume fraction of TiB was fabricated by the powder metallurgy route, and then the elastic modulus and hardness of TiB were measured as 450 and 27.5 GPa (Guojian et al., 2006).

Besides, other methods can also be utilized for obtaining the mechanical properties of TiC and TiB. The elastic modulus and hardness of TiC were calculated as 455 and 32.5 GPa by the first-principle method (Yang et al., 2009). The elastic and shear modulus values of TiB were approximately 371 and 140 GPa, and the Poisson's ratio determined on the basis of rule of mixture approximation was 0.16 using a dynamic method based on impulse excitation of vibration (Atri et al., 1999). It was reported the attractive mechanical properties of superior monolithic TiB material, the Vickers hardness $Hv = 19$ GPa, the elastic modulus $E = 427$ GPa, and the fracture toughness $K_{IC} = 5.5$ MPa $m^{1/2}$ (Shawn et al., 2008).The mechanical properties of *in-situ* synthesized TiB–TiB_2 ceramic-matrix composite were studied and the average Vickers hardness of 26.5 GPa, the flexural strength of 661 MPa and the fracture toughness of 6.95 MPa $m^{1/2}$ were obtained (Wang et al., 2009).

According to above literatures, though some works have been carried out about the mechanical properties of single TiC and TiB, there are some aspects should be improved and investigated further. First, most of work focus on the films and coatings, few investigation of microhardness is carried out in metal matrix composite, especially in titanium matrix composite with the co-existence of two kinds of micro-level reinforcements. Second, for different matrix and composite, the microhardness are diverse because of the different physical properties between the matrix and reinforcements. Finally, the microstructure of TiC and TiB obtained by *in-situ* technology in matrix Ti-6Al-4V will be different from that in the films and coatings, including the shapes and sizes.

In addition, because of the high-strength reinforcements embedded in the matrix, and the different shapes and sizes of reinforcements, it is difficult to obtain the hardness values by conventional methods. Moreover, the mechanical properties exhibited by the composite with different volume fractions of reinforcements are different. The hardness of single reinforcement has been investigated and carried out, however, there is no relevant work on the hardness of two reinforcements on one titanium composite. Consequently, the TiC and TiB reinforcements in (TiB+TiC)/Ti-6Al-4V will be fabricated by *in-situ* synthesized technique, and the microhardness of micro-level TiC and TiB will be investigated by nanoindentation method. The microstructure variation will also be illuminated before and after indentation characterization. The related results will be analyzed and discussed in detail. The results of this work will provide a useful reference for the analysis of micromechanical properties of the reinforcement in titanium matrix composites, which also provide an important basis for the characterization and simulation of mechanical properties of composite materials.

EXPERIMENTAL

Preparation of Materials

The TMC of (TiB+TiC)/Ti-6Al-4V [TiB: TiC = 1:1 (vol%)] with 8% volume percentages of reinforcements were manufactured by consumable vacuum arc remelting. Stoichiometric raw materials of sponge titanium, graphite powder and B_4C were melted homogeneously in a consumable vacuum furnace to produce TMC via self-propagation reactions: $5Ti + B_4C = 4TiB + TiC$and $Ti + C = TiC$ (Zhang et al., 1999). The ingots were melted three times for ensuring the chemical homogeneity, and then hot-forged into a rod with diameter of 20 mm. The samples were obtained from ingots by wire cutting, and the thickness of samples was 3 mm. Before indentation experiment, the samples were grinded and polished.

Nanoindentation Measurement and Microhardness Calculation

The measure of microhardness was performed via the nanoindentation method utilizing indenters (Micro Materials Ltd, UK). Instead of pyramidal indenters, the spherical tip with

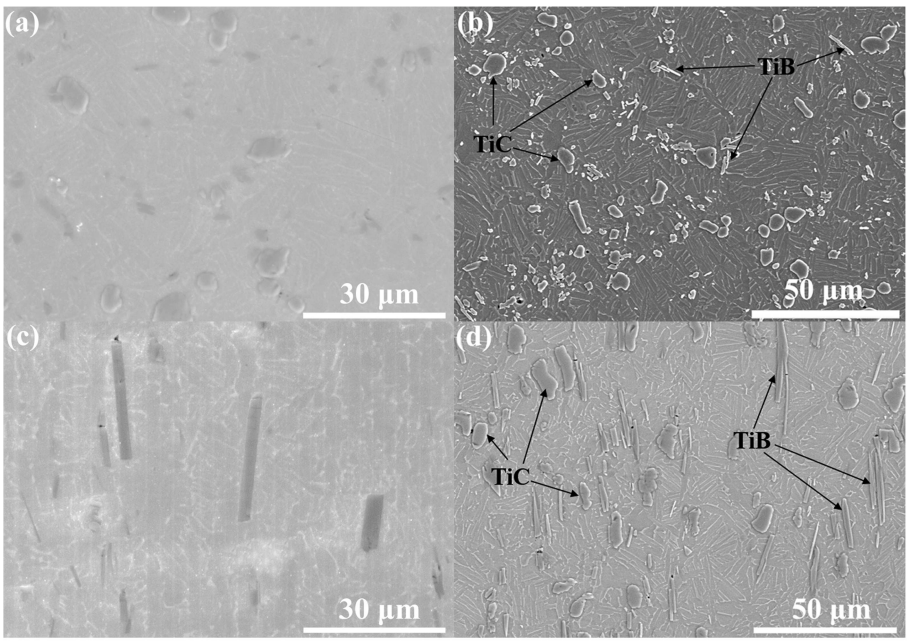

FIGURE 1 | SEM images of the reinforcements. Perpendicular to the axial direction before **(a)** and after **(b)** etching. Parallel to the axial direction before **(c)** and after **(d)** etching.

radius of 10 μm was utilized for measuring in this work to avoid generating cracks, because the stress concentration was not as severe as that created by pyramidal indenter (Fischer-Cripps, 2004). Tests were performed under the closed loop control, the max load were 60 and 20 mN for TiC and TiB, respectively, and the loading rate was 0.01 mN/s. After measuring, the load-displacement curves were obtained, and the microhardness were calculated based on Oliver-Pharr method (Oliver and Pharr, 1992). The area function (A) of spherical tip was corrected before testing, which can be expressed as (Oliver and Pharr, 1992):

$$A = C_1 h_p^2 + C_2 h_p + C_3 h_p^{1/2} + C_4 h_p^{1/4} + C_5 h_p^{1/8} + \cdots \quad (1)$$

where C is the fitting constant and the h_p is the depth of contact of indenter with the specimen. Then the hardness can be calculated as:

$$H = \frac{P}{A} \quad (2)$$

where P is the peak loading. Considering the small size of micro-level TiC and TiB, at least 10 tests were performed on each condition. All measurements were implemented at room temperature.

Microstructure Characterization

Microstructure characterization of reinforcements before and after testing were performed utilizing scanning electron microscope (SEM, Hitachi S-3400N, Japan). The surface morphology and roughness of samples were measured by MicroXAM Surface Mapping Microscope (ADE Phase Shift, USA). Specimens were cut from the hot-forged rods along the axial and radial direction. Before indentation experiment, the specimens were orderly grinded by different abrasive papers (400 + 600 + 800 grit), and then polished using 9 and 3 μm diamond suspensions, and finally polished by 0.05 μm aluminum oxide suspension. Meanwhile, the indenter was cleaned by ethanol in ultrasonic container for 10 mins. After nanoindentation experiment, the surface of specimens were cleaned by acetone and ethanol by ultrasonic for 10 mins to clean the contaminations. For acquiring the accurate size and clear distribution of reinforcements, some specimens were etched using Kroll's solution [HF: HNO_3: H_2O = 3: 5: 92 (vol)] for 2–6 s after polishing. All experiments were carried out at room temperature.

RESULTS AND DISCUSSION

Microstructure of Reinforcements

SEM images about the distribution of reinforcements in (TiB+TiC)/Ti-6Al-4V paralleling and perpendicular to the axial direction are shown in **Figure 1**. **Figures 1a,c** represent the unetched surfaces. There are two types of reinforcements showing different morphologies. The microstructure of etched surfaces are shown in **Figures 1b,d**. The matrix is homogeneous with α (gray, online) and β (white, online) phases, and the reinforcements are distributed uniformly. The reinforcements with needle-, whisker- and short fiber-shaped are TiB. And the equiaxed or near equiaxed shape, and particle-shaped reinforcements are TiC. The different solidification path and crystal structure causes the diverse morphology of

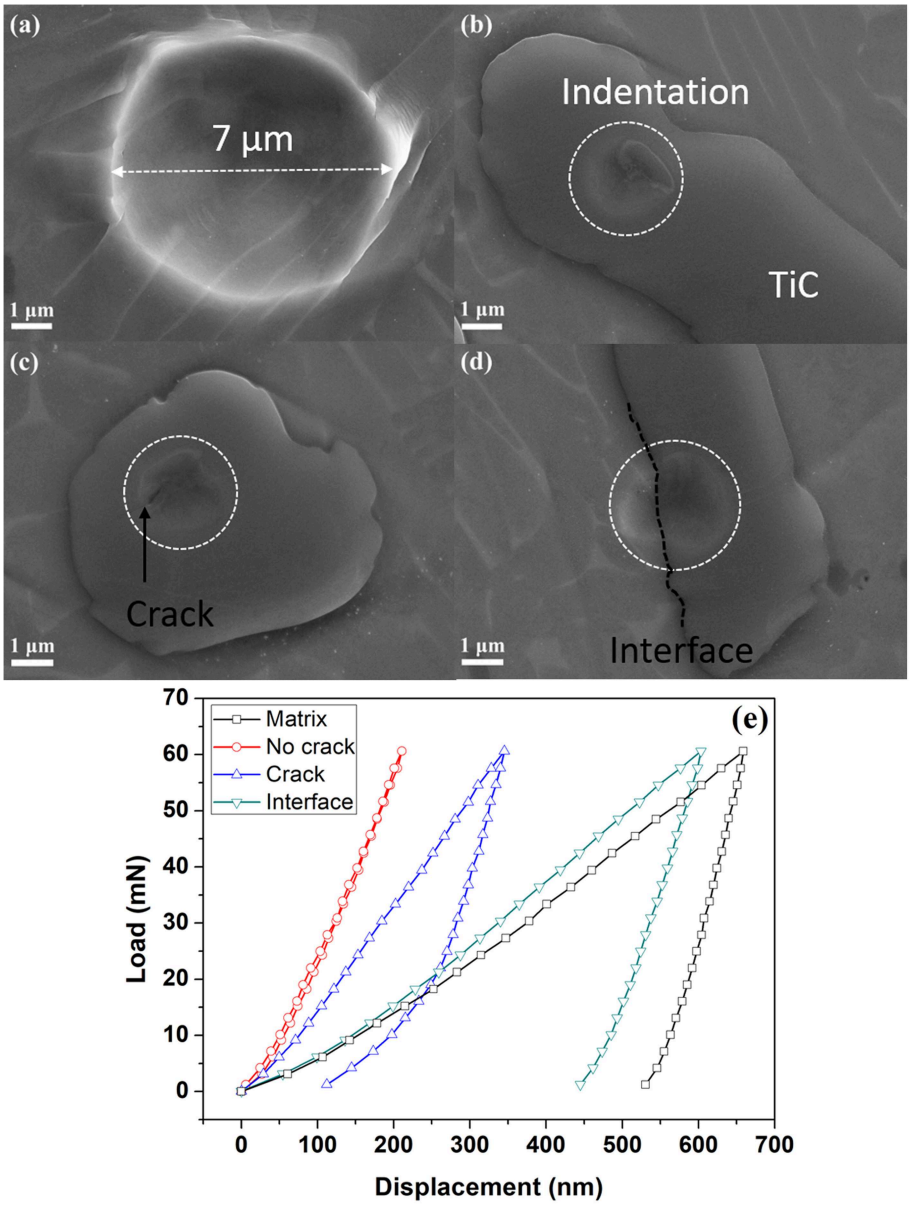

FIGURE 2 | SEM images of indentation and the load-displacement curves under 60 mN: **(a)** indentation on matrix without cracks; **(b)** indentation on TiC without cracks; **(c)** indentation on TiC with cracks; **(d)** indentation on the interface; **(e)** the load-displacement curves.

reinforcements (Lu et al., 2001a). Comparing **Figures 1b,d**, it can be found that the distribution of reinforcements are different along two directions, especially TiB whiskers. The generated TiB are nearly parallel to the axial direction because of the realignment during hot forging (the axial direction is the hot-forging direction). However, there is no obvious effect on TiC particles since the shapes of TiC are globular, near globular or ellipsoid. The total volume fraction of reinforcements in TMC is 8%. According to the calculation before materials preparation, the volume fraction of TiB and TiC are 4%, respectively. Due to the diversification of shape and size of TiC and TiB, it is difficult to accurately determine the volume of each reinforcement. The volume of TiC and TiB under the indentation can be approximatively calculated. TiC is equivalent to a spherical shape, and the average diameter is about 7 μm. TiB is equivalent to a long column shape, and the average diameter is about 3 μm.

Nanoindentation Analysis on Matrix and Reinforcements

The SEM images of indented imprint on matrix and TiC reinforcements are shown in **Figure 2** for the case of peak loading at 60 mN. According to the relevant references (Lu et al., 2001a,b,c), the interface between reinforcements (TiC and TiB)

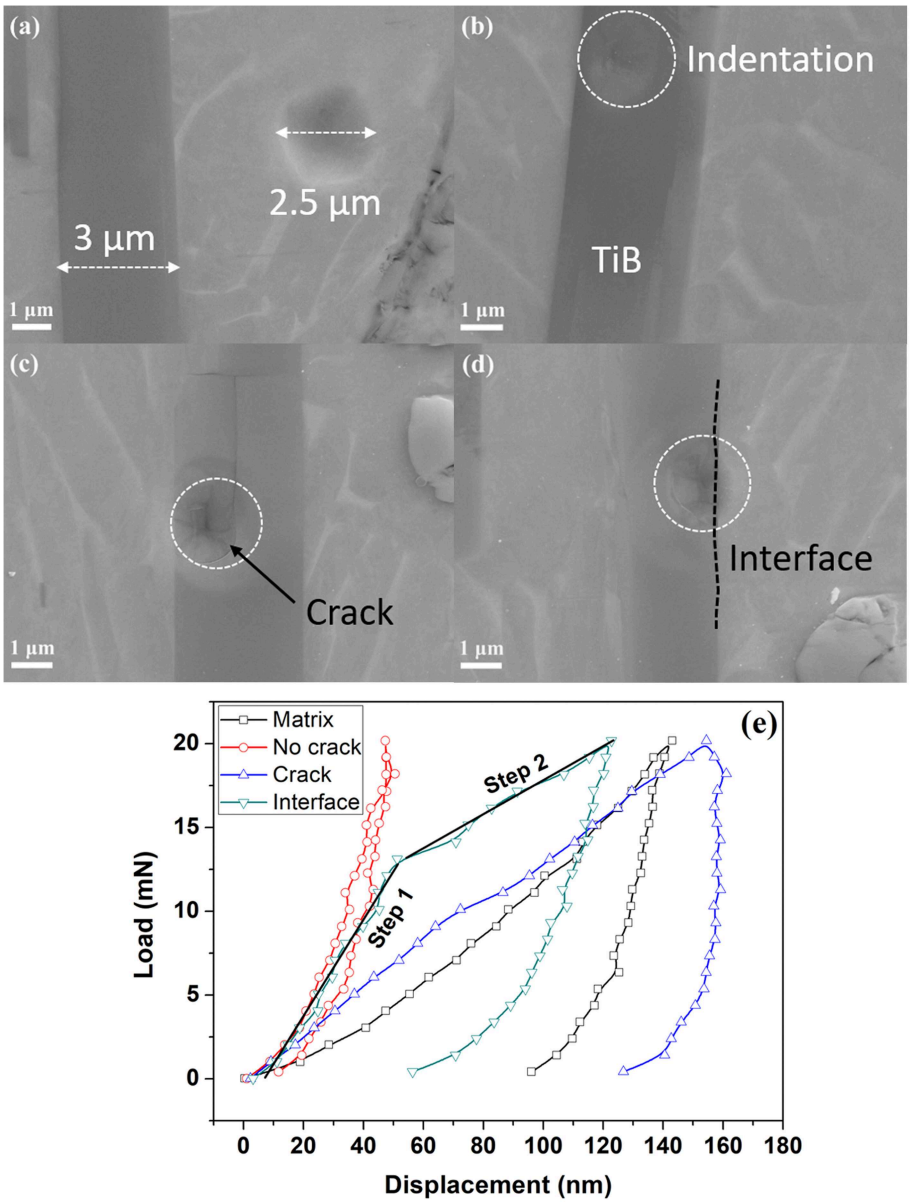

FIGURE 3 | SEM images of indentation and the load-displacement curves under 20 mN: **(a)** indentation on matrix without cracks; **(b)** indentation on TiB without cracks; **(c)** indentation on TiB with cracks; **(d)** indentation on the interface; **(e)** the load-displacement curves.

and matrix can be completely distinguished. TiC are globular and ellipsoid, and TiB are holding a needle like geometry, the interface between TiC and matrix is smooth arc, but the interface between TiB and matrix is straight and flat. Based on above analysis, the labels in **Figure 2** are actually similar as those in **Figure 1**, which are reasonable, just the reinforcements are magnified. It can be found that the diameter of indentation on matrix is about 7 μm (**Figure 2a**), and there is no crack. The plastic deformation inside and around the impression are observed. **Figure 2b** indicates the indentation on TiC, and the diameter of indentation is about 2 μm. Because of the higher microhardness and elasticity modulus of reinforcements, the diameter of indentation is samller than that on matrix. Cracks also can be observed on some indented TiC particles (**Figure 2c**). **Figure 2d** shows one of examples that indented on the TiC/matrix interface. The surface of reinforcement is slightly higher than the matrix. It is supposed that the indenter indented on the reinforcemnet first, and then indented on the matrix as following. In order to obtain the microhardness of TiC, the load-diaplacement curves at above four conditions are shown in **Figure 2e**. In **Figure 2e**, the depths of indentation are shown clearly, and the depth of indentation on TiC without crack is only 210 nm, but which on the matrix reaches 658 nm. The indentation depth on TiC with cracks and interface are 345

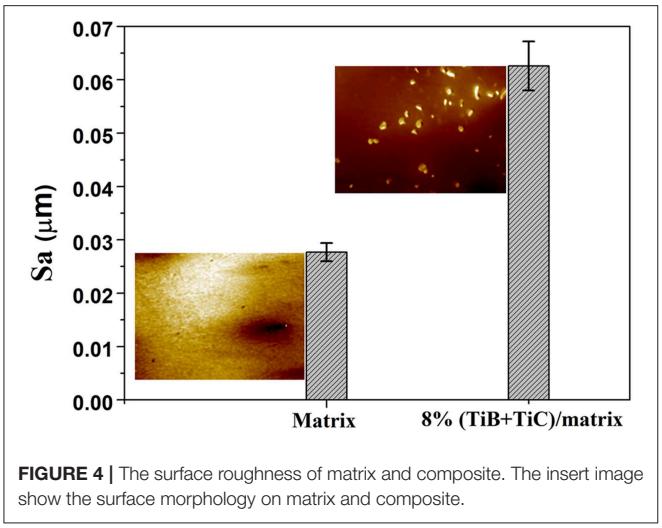

FIGURE 4 | The surface roughness of matrix and composite. The insert image show the surface morphology on matrix and composite.

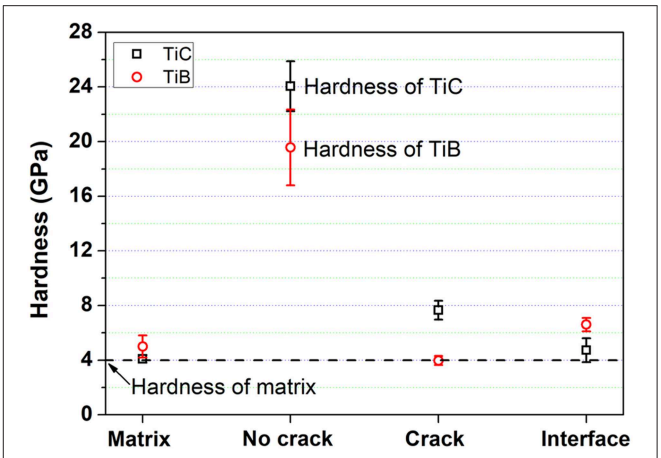

FIGURE 5 | Microhardness of matrix, TiC and TiB at four different conditions.

and 600 nm, respectively. Moreover, it indicates that the slopes of load-displacement curves are different, especially between the indentation on TiC without crack and the matrix. The different slops reveal the different micorhardness at these four conditions. The calculated microhardness will be analyzed in the following section.

Figure 3 shows the morphology of indentation on the matrix and TiB. A lower peak loading of 20 mN is applied, because of the smaller size of TiB and its brittle property compared to TiC. In **Figure 3a**, the diameter of indentation on matrix is reduced to 2.5 μm, which caused by the reduced load. **Figure 3b** shows the case of indentation on TiB without cracks, and the diameter of indentation is about 1.5 μm. Because of the brittless of TiB, the cracks appear on some cases and the crack is propogated under loading (**Figure 3c**). It seems that the cracks radiate from the center of indentation due to the possible stress concentration on the indentation axis. **Figure 3d** shows the indentation on the TiB/matrix interface. The phenomena is similar to that indented on TiC. The spherical tip indented on TiB firstly and then on the matrix. The load-diaplacement curves are shown in **Figure 3e**.

In **Figure 3e**, the depth of indentation on TiB without crack is only 50 nm, but that in the matrix is about 150 nm. Besides, the depth of indentation on TiB with cracks is maximum at 160 nm, which is different from that on TiC (**Figure 2e**), this phenomena may be caused by the large number of cracks on TiB during loading (**Figure 3c**), and moreover, the propogation of cracks results in the fast penetration of indenter on the surface of TiB. In addition, there are two steps (step 1 and 2) of loading on the TiB/matrix interface in **Figure 3e**, step 1 is corresponding to the process of indenter pressing on TiB firstly, and then step 2 represents the process of indenter pressing on the matrix, which are agree well with the analysis of **Figure 3d**. However, these two steps on the interface between TiC and matrix are not obvious in **Figure 2e**, because the load on TiC is 60 mN, which is larger enough to eliminate the difference of height between TiC and matrix. Comparing **Figures 2e**, **3e**, when the loading force is 60 mN, the step cannot be observed at the interface. While the loading force is decreased to 20 mN, the step appears, indicating that the step is influenced by the magnitude of the loading force. If the loading force is too small, the step will influence the hardness of interface. If the loading force is much larger, the step will not affect the hardness of interface. Besides, this work focuses on the hardness variation of the reinforcement, and the hardness on reinforcement/matrix interface is not only influenced by the hardness of reinforcement and matrix, but also affected by the step, which will be studied in the subsequent work. The loading force will be adjusted in turn to analyze the relationship between the loading force and the hardness of interface.

In order to quantify the height difference between the matrix and reinforcements, the approximate height difference can be obtained according to the difference of surface roughness between matrix and reinforcements. The surface morphology and roughness of samples are tested by MicroXAM Surface Mapping Microscope (ADE Phase Shift, USA). The parameters of average roughness *Sa* are defined in Equation (3) (Image Metrology, 2013). The values of *Sa* can reveal the statistical average roughness of surface.

$$S_a = \frac{1}{MN} \sum_{k=0}^{M-1} \sum_{l=0}^{N-1} |z(x_k, y_l) \tag{3}$$

M and *N* represent the number of contour points in *x* and *y* direction, respectively, $z(x_k,y_l)$ is the contour height of each point. In this work, the variation of surface roughness between matrix and composite are shown in **Figure 4**. From **Figure 4**, it can be found that the average difference of roughness is about 35 nm, which means the average height difference between matrix and reinforcement is about 35 nm. It is much smaller than the depth of indentation (∼ 110 nm), consequently, the height difference does not influence the experiment of indentation.

Microhardness Analysis on Matrix and Reinforcements

The microhardness of matrix, TiC and TiB are calculated and shown in **Figure 5**. The microhardness of matrix is about 4 GPa, but the average values of TiC and TiB are 24.1 and 19.6

GPa, respectively. The microhardness of reinforcement with cracks during loading ranges from 4 to 8 GPa, which is much smaller than that of reinforcements because of the cracks. The microhardness on reinforcement/matrix interface is between 4 to 7 GPa, which is contributed by both the matrix and reinforcements. The hardness of reinforcement/matrix interface is not only influenced by the hardness of reinforcement and matrix, but also related to other factors, such as the step, the relative ratio of the indentation area by indenter on the reinforcement and matrix (S_{TiB}/S_{matrix} or S_{TiC}/S_{matrix}). Because the hardness of reinforcement is significantly higher than that of the matrix, if the relative indentation area shows a large proportion on the reinforcements, the hardness measured on the interface will be increased. On the contrary, if the relative indentation area shows a small proportion on the reinforcements, the hardness value measured on the interface will be decreased. Comparing **Figures 2d**, **3d**, it can be found that the relative indentation area on TiB shows a larger proportion than that on TiC ($S_{TiB}/S_{matrix} > S_{TiC}/S_{matrix}$), thus the hardness on TiB/matrix interface is higher than that of TiC/matrix. Consequently, in **Figure 5**, at the interface, the hardness of TiB/matrix interface surpasses that of TiC hardness, the main reason is that during the indentation test on the interface, the relative proportion of indentation area on TiB is larger than that on TiC. Yang *et al* and Wang *et al* reported the microhardness values of H for single reinforcement phases as $H_{\mathrm{TiC}} = 32.5$ GPa (Yang et al., 2009), and $H_{\mathrm{TiB}} = 17.3$ GPa (the middle of range 13.8–20.8 GPa) (Wang et al., 2009), respectively. Comparing to these results, it can be elucidated that the microhardness of TiC and TiB in (TiC+TiB)/Ti-6Al-4V are similar with the results in some other composite and coating materials. It is also verified that the method of nanoindentation is a very useful method to characterize the microhardness of reinforcements in discontinuous metal matrix composite.

CONCLUSIONS

The microhardness of TiC and TiB in (TiC+TiB)/Ti-6Al-4V were investigated by nanoindentation method. Some useful results were obtained and elucidated.

(1) According to the indentation on matrix, TiC and TiB, the cracks appeared on some TiC and TiB reinforcements, which influenced the value of microhardness. The reasonable microhardness could be calculated from the load-displacement curves without cracks.
(2) The load-displacement curves on the reinforcement/matrix interface showed two steps on loading. Step 1 was corresponding to the process of indenter pressing on reinforcement firstly, and then step 2 represented the process of indenter pressing on matrix, which caused by the height difference between reinforcements and matrix.
(3) The height difference between the matrix and reinforcements could be obtained according to the difference of surface roughness between matrix and reinforcements. The average height difference was about 35 nm, which was much smaller than the depth of indentation, consequently, the height difference did not influence the experiment of indentation.
(4) The average microhardness of TiC and TiB were 24.1 and 19.6 GPa, respectively, which were similar with those in some other materials. It was verified the method of nanoindentation was a useful method to characterize the microhardness of reinforcements in discontinuous metal matrix composite.

DATA AVAILABILITY

The raw data supporting the conclusions of this manuscript will be made available by the authors, without undue reservation, to any qualified researcher.

AUTHOR CONTRIBUTIONS

YW and TG designed and carried out the experiments. YZ and HB assisted with the materials characterization. ZW provided the idea and assisted with the discussion on results. YW and TG wrote the main manuscript text.

FUNDING

This work was financial supported by Fundamental Research Funds for the Central Universities (WUT 2018IVA063, WUT 2018IVA064), Chu Tian Scholar project of Hubei Province (CTXZ2017-05), and the 111 Project (B17034).

REFERENCES

Atri, R. R., Ravichandran, K. S., and Jha, S. K. (1999). Elastic properties of *in-situ* processed Ti–TiB composites measured by impulse excitation of vibration. *Mater. Sci. Eng. A* 271, 150–159. doi: 10.1016/S0921-5093(99)00198-7

Banerjee, R., Genç, A., Collins, P. C., and Fraser, H. L. (2004). Comparison of microstructural evolution in laser-deposited and arc-melted *in-situ* Ti-TiB composites. *Metallurg. Mater. Trans. A* 35, 2143–2152. doi: 10.1007/s11661-004-0162-0

Cheng, J., Liu, D., Liang, X., and Chen, Y. (2015). Evolution of microstructure and mechanical properties of *in situ* synthesized TiC–TiB_2/CoCrCuFeNi high entropy alloy coatings. *Surf. Coat. Technol.* 281, 109–116. doi: 10.1016/j.surfcoat.2015.09.049

Constantinides, G., Ravi Chandran, K. S., Ulm, F. J., and Van Vliet, K. J. (2006). Grid indentation analysis of composite microstructure and mechanics: principles and validation. *Mater. Sci. A* 430, 189–202. doi: 10.1016/j.msea.2006.05.125

Donohue, B. R., Ambrus, A., and Kalidindi, S. R. (2012). Critical evaluation of the indentation data analyses methods for the extraction of isotropic uniaxial mechanical properties using finite element models. *Acta Mater.* 60, 3943–3952. doi: 10.1016/j.actamat.2012.03.034

Fang, T. H., Jian, S. R., and Chuu, D. S. (2004). Nanomechanical properties of TiC, TiN and TiCN thin films using scanning probe microscopy and nanoindentation. *Appl. Surf. Sci.* 228, 365–372. doi: 10.1016/j.apsusc.2004.01.053

Feng, G., Yang, Y., Luo, X., Li, J., Huang, B., and Chen, Y. (2015). Fatigue properties and fracture analysis of a SiC fiber-reinforced titanium matrix composite. *Compos. Part B Eng.* 68, 336–342. doi: 10.1016/j.compositesb.2014.09.005

Fischer-Cripps, A. C. (2004). *Nanoindentation.* New York, NY: Springer.

Geng, K., Lu, W., Yang, Z., and Zhang, D. (2003). *In situ* preparation of titanium matrix composites reinforced by TiB and Nd_2O_3. *Mater. Lett.* 57, 4054–4057. doi: 10.1016/S0167-577X(03)00264-7

Guojian, C., Lin, G., and Masaaki, N. (2006). Elastic properties of titanium monoboride measured by nanoindentation. *J. Am. Ceram. Soc.* 89, 3836–3838. doi: 10.1111/j.1551-2916.2006.01280.x

Huang, L., and Geng, L. (2017). *Discontinuously Reinforced Titanium Matrix Composites.* Singapore: Springer; National Defense Industry Press, Beijing and Springer Nature Singapore Pte Ltd.

Huang, L., Geng, L., and Peng, H. (2015). Microstructurally inhomogeneous composites: is a homogeneous reinforcement distribution optimal? *Prog. Mater. Sci.* 71, 93–168. doi: 10.1016/j.pmatsci.2015.01.002

Image Metrology (2013). *The Scanning Probe Image Processor.* SPIPTM, User's and Reference 4. Available online at: https://www.imagemet.com/

Koo, M. Y., Park, J. S., Park, M. K., Kim, K. T., and Hong, S. H. (2012). Effect of aspect ratios of *in situ* formed TiB whiskers on the mechanical properties of TiB_w/Ti−6Al−4V composites. *Scr. Mater.* 66, 487–490. doi: 10.1016/j.scriptamat.2011.12.024

Lu, W., Zhang, D., Zhang, X., Bian, Y., Wu, R., Sakata, T., et al. (2001a). Microstructure and tensile properties of *in situ* synthesized (TiBw + TiCp)/Ti6242 composites. *J. Mater. Sci.* 36, 3707–3714. doi: 10.1023/A:1017917631855

Lu, W., Zhang, D., Zhang, X., Wu, R., Sakata, T., and Mori, H. (2001b). HREM study of TiB/Ti interfaces in a TiB-TiC *in situ* composite. *Scr. Mater.* 44, 1069–1075. doi: 10.1016/S1359-6462(01)00663-7

Lu, W., Zhang, D., Zhang, X., Wu, R., Sakata, T., and Mori, H. (2001c). Microstructural characterization of TiB in *in situ* synthesized titanium matrix composites prepared by common casting technique. *J. Alloys Compd.* 327, 240–247. doi: 10.1016/S0925-8388(01)01445-1

Maerky, C., Guillou, M. O., Henshall, J. L., and Hooper, R. M. (1996). Indentation hardness and fracture toughness in single crystal TiC0.96. *Mater. Sci. Eng. A* 209, 329–336. doi: 10.1016/0921-5093(95)10152-7

Oliver, W. C., and Pharr, G. M. (1992). Improved technique for determining hardness and elastic modulus using load and displacement sensing indentation experiments. *J. Mater. Res.* 7, 1564–1583. doi: 10.1557/JMR.1992.1564

Oliver, W. C., and Pharr, G. M. (2004). Measurement of hardness and elastic modulus by instrumented indentation: advances in understanding and refinements to methodology. *J. Mater. Res.* 19, 3–20. doi: 10.1557/jmr.2004.19.1.3

Rastegari, H., and Abbasi, S. M. (2013). Producing Ti−6Al−4V/TiC composite with superior properties by adding boron and thermo-mechanical processing. *Mater. Sci. Eng. A* 564, 473–477. doi: 10.1016/j.msea.2012.12.011

Saito, T., Furuta, T., and Yamaguchi, T. (1995). "Development of low cost titanium alloy matrix composite," in *Recent Advances in Titanium Metal Matrix Composites* (Warrendale, PA: TMS), 33–44.

Schuh, C., and Dunand, D. C. (2001). Whisker alignment of Ti−6Al−4V/TiB composites during deformation by transformation superplasticity. *Int. J. Plasticity* 17, 317–340. doi: 10.1016/S0749-6419(00)00038-3

Sekkal, W., Zaoui, A., and Schmauder, S. (2005). Nanoindentation study of the superlattice hardening effect at TiC(110)/NbC(110) interfaces. *Appl. Phys. Lett.* 86, 163108-163183. doi: 10.1063/1.1897432

Shawn, M., Curtis, L., and S., R.C.K. (2008). Physical and mechanical properties of nanostructured titanium boride (TiB) ceramic. *J. Am. Ceram. Soc.* 91, 1319–1321. doi: 10.1111/j.1551-2916.2007.02246.x

Sun, S., Wang, M., Wang, L., Qin, J., Lu, W., and Zhang, D. (2012). The influences of trace TiB and TiC on microstructure refinement and mechanical properties of *in situ* synthesized Ti matrix composite. *Compos. Part B Eng.* 43, 3334–3337. doi: 10.1016/j.compositesb.2012.01.075

Tjong, S. C., and Ma, Z. (2000). Microstructural and mechanical characteristics of *in situ* metal matrix composites. *Mater. Sci. Eng. Rep.* 29, 49–113. doi: 10.1016/S0927-796X(00)00024-3

Tjong, S. C., Ma, Z. Y., and Li, R. K. Y. (1999). The dynamic mechanical response of Al_2O_3 and TiB_2 particulate reinforced aluminum matrix composites produced by *in-situ* reaction. *Mater. Lett.* 38, 39–44. doi: 10.1016/S0167-577X(98)00129-3

Tu, J. P., Wang, N. Y., Yang, Y. Z., Qi, W. X., Liu, F., Zhang, X. B., et al. (2002). Preparation and properties of TiB_2 nanoparticle reinforced copper matrix composites by *in situ* processing. *Mater. Lett.* 52, 448–452. doi: 10.1016/S0167-577X(01)00442-6

Wagoner Johnson, A. J., Kumar, K. S., and Briant, C. L. (2003). Deformation mechanisms in Ti-6Al-4V/TiC composites. *Metallurg. Mater. Trans. A* 34, 1869. doi: 10.1007/s11661-003-0152-7

Wang, F.-C., Zhang, Z. H., Luo, J., Huang, C.-C., and Lee, S.-K. (2009). A novel rapid route for *in situ* synthesizing TiB–TiB_2 composites. *Compos. Sci. Technol.* 69, 2682–2687. doi: 10.1016/j.compscitech.2009.08.010

Wang, L., Xie, L., Lv, Y., Zhang, L.-C., Chen, L., Meng, Q., et al. (2017). Microstructure evolution and superelastic behavior in Ti-35Nb-2Ta-3Zr alloy processed by friction stir processing. *Acta Mater.* 131, 499–510. doi: 10.1016/j.actamat.2017.03.079

Wang, L., Xie, L., Shen, P., Fan, Q., Wang, W., Wang, K., et al. (2019). Surface microstructure and mechanical properties of Ti-6Al-4V/Ag nanocomposite prepared by FSP. *Mater. Charact.* 153, 175–183. doi: 10.1016/j.matchar.2019.05.002

Wang, M., Lu, W., Qin, J., Zhang, D., Ji, B., and Zhu, F. (2005). Superplastic behavior of *in situ* synthesized (TiB+ TiC)/Ti matrix composite. *Scr. Mater.* 53, 265–270. doi: 10.1016/j.scriptamat.2005.01.049

Wei, Z., Cao, L., Wang, H., and Zou, C. (2011). Microstructure and mechanical properties of TiC/Ti-6Al-4V composites processed by *in situ* casting route. *Mater. Sci. Technol.* 27, 1321–1327. doi: 10.1179/026708310X12699498462922

Xie, L., Jiang, C., Lu, W., Chen, Y., and Huang, J. (2012). Effect of stress peening on surface layer characteristics of (TiB + TiC)/Ti−6Al−4V composite. *Mater. Des.* 33, 64–68. doi: 10.1016/j.matdes.2011.07.010

Xie, L., Wang, L., Jiang, C., and Lu, W. (2014). The variations of microstructures and hardness of titanium matrix composite (TiB+ TiC)/Ti−6Al−4V after shot peening. *Surf. Coat. Technol.* 244, 69–77. doi: 10.1016/j.surfcoat.2014.01.053

Xie, L., Wang, L., Wang, K., Yin, G., Fu, Y., Zhang, D., et al. (2018a). TEM characterization on microstructure of Ti−6Al−4V/Ag nanocomposite formed by friction stir processing. *Materialia* 3, 139–144. doi: 10.1016/j.mtla.2018.08.007

Xie, L., Wang, Z., Wang, C., Wen, Y., Wang, L., Jiang, C., et al. (2018b). "Finite element dynamic analysis on residual stress distribution of titanium alloy and titanium matrix composite after shot peening treatment," in *Finite Element Method: Simulation, Numerical Analysis and Solution Techniques*, ed P. Răzvan (London: IntechOpen Publisher), 23–48.

Yang, Y., Lu, H., Yu, C., and Chen, J. M. (2009). First-principles calculations of mechanical properties of TiC and TiN. *J. Alloys Compd.* 485, 542–547. doi: 10.1016/j.jallcom.2009.06.023

Zhang, L.-C., and Attar, H. (2016). Selective laser melting of titanium alloys and titanium matrix composites for biomedical applications: a review. *Adv. Eng. Mater.* 18, 463–475. doi: 10.1002/adem.201500419

Zhang, L.-C., Xu, J., and Eckert, J. (2006). Thermal stability and crystallization kinetics of mechanically alloyed TiC/Ti-based metallic glass matrix composite. *J. Appl. Phys.* 100:033514. doi: 10.1063/1.2234535

Zhang, L. C., and Chen, L.-Y. (2019). A review on biomedical titanium alloys: recent progress and prospect. *Adv. Eng. Mater.* 21:1801215. doi: 10.1002/adem.201801215

Zhang, L. C., Liu, Y., Li, S., and Hao, Y. (2018). Additive manufacturing of titanium alloys by electron beam melting: a review. *Adv. Eng. Mater.* 20:1700842. doi: 10.1002/adem.201700842

Zhang, X., Lü, W., Di, Z., Wu, R., Bian, Y., and Fang, P. (1999). *In situ* technique for synthesizing (TiB+TiC)/Ti composites. *Scr. Mater.* 41, 39–46. doi: 10.1016/S1359-6462(99)00087-1

Conflict of Interest Statement: The authors declare that the research was conducted in the absence of any commercial or financial relationships that could be construed as a potential conflict of interest.